

Generation and Investigation of Number States of the Radiation Field¹

Herbert Walther

*Sektion Physik der Universität München
and Max-Planck-Institut für Quantenoptik
85748 Garching, Fed. Rep. of Germany*

Abstract

The widely discussed applications in quantum information and quantum cryptography require radiation sources capable of producing a fixed number of photons. This paper reviews the work performed in our laboratory to produce these fields on demand. Two different methods are discussed. The first is based on the one-atom maser or micromaser operating under the conditions of the so-called trapping states. In this situation the micromaser stabilises to a photon number state. Recently, we also succeeded in determining the Wigner function of a single-photon state. The second device, recently realised in our laboratory, uses a single trapped ion in an optical cavity.

1 Introduction

The quantum treatment of the radiation field uses the number of photons in a particular mode to characterise the quantum states. The ground state of the quantum field is represented by the vacuum state consisting of field fluctuations with no residual energy. The states with fixed photon number are usually called Fock or number states. They are used as a basis on which any general radiation field state can be expressed. Fock states thus represent the most basic quantum states and maximally differ from what one would call a classical field. Although Fock states of vibrational motion are routinely observed, e.g. in ion traps [1], Fock states of the radiation field are very fragile and very difficult to produce and maintain. They are perfectly number-squeezed, extreme sub-Poissonian states in which intensity fluctuations completely vanish.

The special case of single-photon fields are necessary for secure quantum communication [2, 3, 4] and quantum cryptography [5] and are also required in some cases for quantum computing [6]. Photon fields with fixed photon numbers are also interesting from the point of view of fundamental physics since they represent, as pointed out above, the ultimate non-classical limit of radiation. When the photon number state is produced by strong coupling of excited-state atoms, a corresponding number of ground-state atoms is simultaneously populated. Such a system therefore produces a fixed number of atoms in the lower state as well. This type of atom source is a long sought after *gedanken* device as well [7]. Single photons have been generated by several processes such as single-atom fluorescence [8, 9, 10], single-molecule fluorescence [11], two-photon down-conversion [12], and Coulomb blockade of electrons [13], and one- and two-photon Fock states have been generated in the micromaser [14, 15]. As these sources do not produce photons on demand, they are better described as “heralded” photon sources, because they are stochastic either in the emission direction or in the time of creation. A source of single photons or, more generally, of Fock states

¹In collaboration with S. Brattke, G.R. Guthöhrlein, M. Keller, W. Lange, and B. Varcoe

generated on demand has just recently been demonstrated in our laboratory. Cavity quantum electrodynamics (QED) provides us with the possibility of generating a photon both at a particular time and with a predetermined direction. To this end there have been several proposals making use of high-Q cavities, which are basically capable of serving as sources of single photons [4, 16, 17, 18]. The current paper reviews the work on a microwave source capable of producing a preset number of photons and lower state atoms. The principle of the source and the experimental demonstration will be described. It is based on the One-Atom Maser or micromaser and allows a specified photon Fock state ($n \geq 1$) to be generated *on demand*, without need of conditional measurements, thus making it independent of detector efficiencies.

The second part of the paper describes the work towards a new single-photon source in the visible spectral range. This source uses a single trapped ion placed in a cavity. The realisation of this source is reported.

Steady-state operation of the One-Atom Maser has been extensively studied both theoretically [19] and experimentally, and has already been used to demonstrate many quantum phenomena of the radiation field such as sub-Poissonian statistics [20], collapse and revival of Rabi oscillations [21], and entanglement between the atoms and cavity field [22]. More recently, two experiments demonstrated that Fock states (i.e. states with a fixed photon number) can readily be created in normal operation of the maser by means of either state reduction [14] or steady-state operation of the micromaser in a trapping state [15]. The trapping states in the micromaser are the quantum states of the radiation field produced in the maser cavity. They are described in detail below. State reduction is possible owing to entanglement between the state of the outgoing atoms and the cavity field; detection of a lower state atom means that a field originally in an n -photon Fock state is projected onto the $n + 1$ state [23]. As a source of single photons, such a source can be compared to two-photon down-conversion, in which an idler beam is used to prove the creation of a photon in the signal beam. Both are subject to the same limitation in that the creation of the Fock state is unpredictable, and imperfect detectors further reduce the probability of the preparation of such a state. In contrast, it is shown here that the micromaser can be used to prepare Fock states *on demand* with small photon numbers in the cavity. Simultaneously, an equal number of ground state atoms are produced with an efficiency of up to 98%.

Trapping states are a feature of low-temperature operation of the micromaser, for which the steady-state photon distribution closely approximates a Fock state under certain conditions. They are typical of strongly coupled systems. They occur when atoms perform an integer number k of Rabi cycles under the influence of a fixed photon number n :

$$\sqrt{n+1}gt_{\text{int}} = k\pi, \quad (1)$$

where g is the effective atom-field coupling constant and t_{int} is the interaction time. Trapping states are characterised by the number of photons n and the number of Rabi cycles k . The trapping state $(n, k)=(1, 1)$ therefore refers to the one-photon, one-Rabi-oscillation trapped field state. In other words, trapping states occur when the interaction time is chosen such that the emission probability becomes zero for certain operating parameters of the maser. When the trapping state is reached in steady-state operation, the micromaser field will become stabilised. The particular Fock state is known and is determined by the interaction time between the atom and cavity as given by the trapping state formula (Eq. 1). The Fock state, once prepared, is preserved owing to the trapping condition with a minimum probability of photon

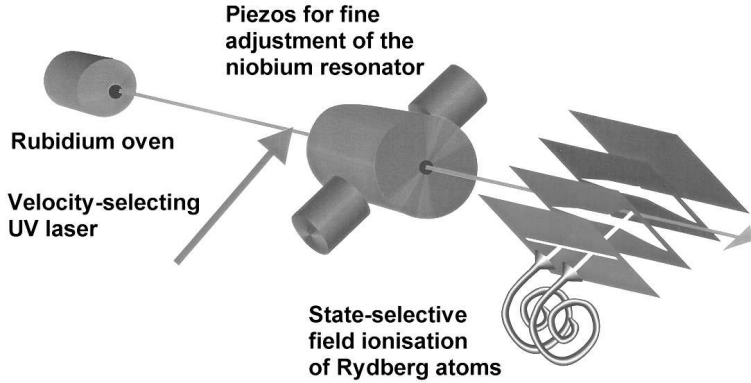


Figure 1: The atoms leaving the rubidium oven are excited into the $63P_{3/2}$ Rydberg state by means of a UV laser at an angle of 11° . After the cavity the atoms are detected by state-selective field ionisation. The cavity is tuned with two piezo translators. An auxiliary atomic beam (not shown) is used to stabilise the laser frequency. The laser is locked to a Stark-shifted atomic resonance of the auxiliary beam, thus allowing the velocity subgroup selected by excitation to be continuously changed within the range of the velocity distribution of the atoms.

emission. Following preparation of the state, the beam of pump atoms can be turned off and the Fock state remains in the cavity for the duration of the cavity decay time. For simplicity, we concentrate in the following on preparation of a one-photon Fock state, but the method can also be generalised to generation of fields of higher photon numbers.

The micromaser setup used for the experiments is shown in Fig. 1 and is operated in the same way as described in [15]. Briefly, a ^3He - ^4He dilution refrigerator houses the closed superconducting microwave cavity. A rubidium oven provides two collimated atomic beams: the main beam passing directly into the cryostat and the second being used to stabilise the laser frequency [15]. (For simplicity, this second beam is not shown in Fig. 1). A frequency-doubled dye laser ($\lambda = 297 \text{ nm}$) was used to excite rubidium (^{85}Rb) atoms to the Rydberg $63P_{3/2}$ state from the $5S_{1/2}(F = 3)$ state. The cavity is tuned to the 21.456 GHz transition from the $63P_{3/2}$ state to the $61D_{5/2}$ state, which is the lower or ground state of the maser transition. For this experiment a cavity with a Q -value of 4×10^{10} was used, this corresponding to a photon lifetime of 0.3 s. This Q -value is the largest ever achieved in this type of experiments and the photon lifetime is more than two orders of magnitude higher than that of related setups [24]. This cavity is used to study micromaser operation in great detail. To realise the Fock state, it is necessary to switch the excitation of the Rydberg atoms on and off in a predefined pulse sequence; this was achieved by means of an intensity-modulating electro-optical modulator triggered by control software. The pulse duration and pulse separation can both be tailored to the conditions required for the particular experiment.

To demonstrate the principle of this source, Fig. 2 shows a sequence of twenty successive pulses obtained by Monte Carlo simulation [25] of the micromaser operating in the $(1, 1)$ trapping state. In each pulse there is a single emission event, producing

a single lower-state atom and leaving a single photon in the cavity. In the case of loss of a photon by dissipation, one of the next incoming excited-state atoms will restore the single-photon Fock state. This condition was observed in [15] when sub-Poissonian atom statistics was measured with the maser operating in a trapping state. The influence of thermal photons and variations in interaction time or cavity tuning further complicates this picture, resulting in reduced visibility of steady-state Fock states [15]. Pulsed excitation as discussed here, however, reduces these perturbations present in the case of continuous operation of the atomic beam and the Fock state is maintained with a high probability [27].

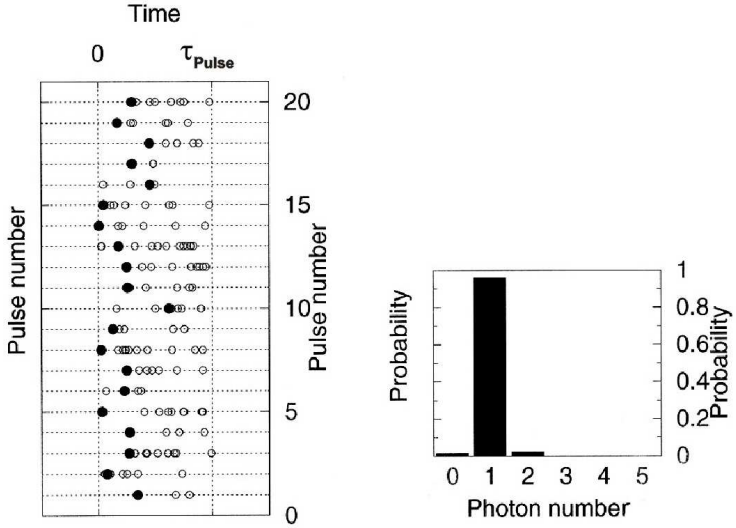


Figure 2: Simulation of a subset of twenty successive atom bunches after the cavity and the associated probability distribution for photons or lower-state atom production (solid circles represent lower-state atoms and blank circles represent excited-state atoms). The start and finish of each pulse are indicated by the vertical dotted lines marked 0 and τ_{pulse} , respectively. The operating conditions are the (1,1) trapping state ($gt_{\text{int}} = 2.2$) conditions. The size of the atoms in this figure is exaggerated for clarity. With the real atomic separation, there is 0.06 atom in the cavity on average (i.e. the system operates in the one-atom regime). The other parameters are $\tau_{\text{pulse}} = 9, 92 \times \tau_{\text{cav}}$, $n_{\text{th}} = 10^{-4}$ and $N_a = 7$ (see also Refs. [26] and [27]).

Figure 3 shows three curves, again obtained from a computer simulation, that illustrate the dynamical behaviour of the maser under pulsed excitation as a function of the interaction time for more ideal (but achievable) experimental parameters. The simulations show the probability of finding no ground-state atom per pulse ($P^{(0)}$) and exactly one ground-state atom per pulse ($P^{(1)}$); and the conditional probability of finding a second ground-state atom in a pulse, if one has already been detected ($P^{(>1;1)}$). The latter plot of the conditional probability, $P^{(>1;1)}$, has the advantage of being especially suitable for comparing theory and experiment since it is relatively insensitive to the detection probability for atoms in the upper and lower maser levels

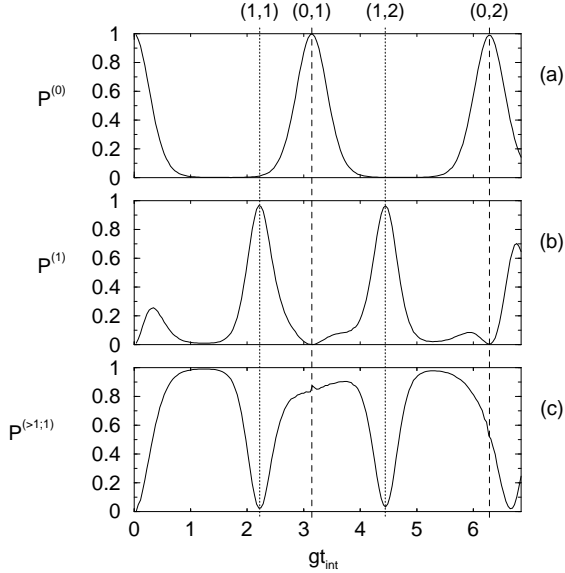


Figure 3: The probability of finding (a) no lower-state atoms per pulse, $P^{(0)}$, (b) exactly one lower-state atom per pulse, $P^{(1)}$, and (c) a second lower-state atom, if one has already been detected, $P^{(>1;1)}$. The parameters are $\tau_{\text{pulse}} = 0.02 \tau_{\text{cav}}$, $N_{\text{a}} = 7$ atoms, and $n_{\text{th}} = 10^{-4}$. The maximum value of $P^{(1)}$ is 98% for the (1, 1) trapping state.

[27].

From the simulations it follows, with an interaction time corresponding to the (1, 1) trapping state, that both one-photon in the cavity and a single atom in the lower state are produced with a 98% probability. In order to maintain an experimentally verifiable quantity, the simulations presented relate to the production of lower-state atoms rather than to the Fock state left in the cavity. Since the duration of the pumping pulses can be kept rather short ($0.01\tau_{\text{cav}} \leq \tau_{\text{pulse}} \leq 0.1\tau_{\text{cav}}$), the dissipation in the cavity can be neglected.

The variation of the time when an emission event occurs during an atom pulse in Fig. 2 is due to the variable time spacing between the atoms as a consequence of Poissonian statistics of the atomic beam and the stochasticity of the quantum process. The atomic rate therefore has to be high enough to ensure a sufficient number of excited atoms per laser pulse, so as to maintain the 98% probability of an atom emitting. To guarantee single-atom single-photon operation, the duration of the preparation pulses must be short in relation to the cavity decay time. For practical purposes, the pulse duration should be smaller than $0.1\tau_{\text{cav}}$ for dissipative losses to be less than 10%.

For a large range of operating conditions, the production of Fock states of the field and single lower-state atoms is remarkably robust against the influence of thermal photons, variations of the velocity of atoms, and other influences such as mechanical vibrations of the cavity; much more so than the steady-state trapping states, for which highly stable conditions with low thermal photon numbers are required [15, 26].

An obvious side-effect of production of a single photon in the mode is, as already mentioned, that a single atom in the lower state is produced. This atom is in a different state when it leaves the cavity, and is therefore distinguishable from the pump atoms. Under these operating conditions, the micromaser thus also serves as a source of single atoms in a particular state, a requirement for many experiments proposed [7, 28].

Our present micromaser setup was specifically designed for steady-state operation and is therefore not ideal for the parameter range presented here. However, the setup does permit comparison between theory and experiment in a relatively small parameter range. With the setup it could be demonstrated that the cavity field is correctly prepared in 83.2% of the pulses [27]. By improving the experimental parameters, we can achieve conditions leading to the expected theoretical result.

One interesting application of the single photon states produced in the micromaser is the determination of the Wigner function of a single photon state giving the phase space distribution of that state. Recently, a new method using the Rabi nutation of atoms in the micromaser was proposed [29]. The method allowed us to use earlier measurements of a single-photon state for evaluation [14]. The value at the origin $W_{|1\rangle}(0) = -1.9$ we got is very close to the theoretically expected value -2.

The second part of this paper reports the progress of our work on ions in optical cavities. The interaction of a single atom with a single field mode of a high-finesse cavity has been the subject of a number of experiments in the field of cavity QED (see, for example, Ref. [18]). However, most of these investigations suffer from a lack of control over the position of the atom, which results in non-deterministic fluctuations of the coupling between atoms and the field. In this context, the strong localisation and position control available when an ion trap is combined with an optical cavity would be a big step forward and would become a key technology for future progress in cavity QED in the optical range. We are now implementing two experiments exploiting localisation of an ion in a cavity. Pulsed excitation of a maximally coupled ion allows single-photon wave packets to be emitted from the cavity on demand [17, 18, 30] (single-photon gun). Under conditions of strong coupling, a single calcium ion in the cavity provides sufficient gain to build up a laser field [16]. Like a single ion in free space, which was previously shown to be an excellent source of antibunched light [9, 10], radiation from a single-ion laser has nonclassical photon statistics and correlations.

An equally attractive goal in the area of cavity QED is the simultaneous interaction of two or more ions with a single-cavity mode. Due to the linear geometry of our trap several ions can be stored within the mode volume. As a first test, we placed an array of two ions in the cavity field and observed the total fluorescence. We succeeded in matching the ion crystal to the two maxima of the TEM₀₁ mode of the cavity. In such a configuration the cavity field may be used to entangle the two ions [31, 32]. This is a promising alternative to schemes involving the ions' motional degrees of freedom, since there is no need for cooling the vibrational modes of the string below the Doppler temperature. Using a cavity to perform quantum operations on adjacent pairs of ions in a long string is a viable route to a scalable quantum computer.

In the following, we now give a progress report of our experiment. (For details see also Ref. [33].) We are using a linear trap with Ca ions (see Fig. 4). As an initial test of the setup for the above-mentioned cavity QED experiments, we used the trapped Ca ions to probe the optical field in the cavity. The Ca ion is sensitive to radiation close to the resonance line $4^2S_{1/2} - 4^2P_{1/2}$ at a wavelength of $\lambda = 397$ nm. The fluorescent light emitted by the ion is collected and detected with a photomultiplier

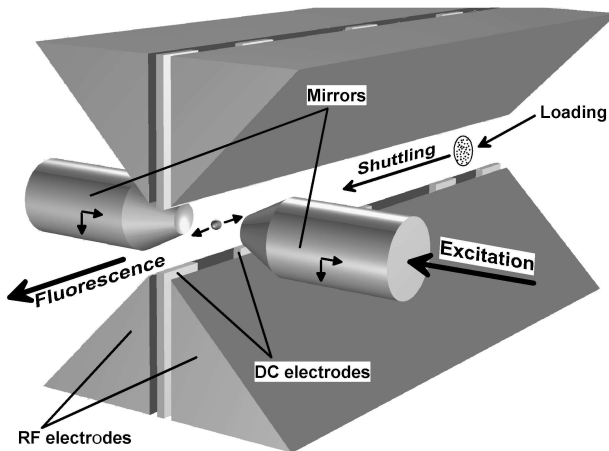


Figure 4: Experimental arrangement of trap electrodes and cavity mirrors. The ion is loaded at the rear end of the trap and shuttled to the mirror region. Fluorescence is observed from the side of the cavity. For scans in the direction of the trap axis, the ion is moved with DC electrodes. In all other directions, the cavity is translated relatively to the ion's position, as indicated by arrows.

tube. The observed fluorescence rate R is proportional to the local intensity of the optical field at the position \vec{r} of the ion, i.e. $R \propto I(\vec{r})$, provided there is no saturation of the atomic transition. By scanning the position of the ion in the field and detecting the fluorescence rate at each point, a high-resolution map of the optical intensity distribution is obtained. It should be noted that a single ion can also probe the amplitude distribution $\vec{E}(\vec{r})$ of the light field and hence measure its phase. To this end, heterodyne detection of the fluorescent light must be used, with the exciting laser as a local oscillator [8, 10].

With the single ion as a probe, we investigated the eigenmodes of a Fabry-Perot resonator formed by two mirrors (radius of curvature = 10 mm) at a distance of $L = 6$ mm (Fig. 4). The transverse mode pattern is described by Hermite-Gauss functions with a beam waist $w_0 \approx 24 \mu\text{m}$, while in the direction of the cavity axis a standing wave builds up. In the experiment, a particular cavity mode is excited by a laser beam with a power of a few hundred nanowatts at 397 nm. The length of the cavity is actively stabilised to this mode.

An ion is loaded in the trap after electron-impact ionisation of calcium atoms. Since the electron beam and the calcium beam would degrade the optical mirrors and make stable trapping difficult, we use a linear trap and load it in a region spatially separated from the observation zone (Fig. 4). Subsequently, DC electrodes along the axis are employed to shuttle the ion over a distance of 25 mm to the uncontaminated end of the trap, where the cavity is located, oriented at right angles to the trap axis. Residual DC fields in the radial direction must be carefully compensated with correctional DC voltages to place the ion precisely on the nodal line of the RF field (coinciding with the trap axis), so as to prevent the trapping field from exciting the micromotion of the ion.

In the direction of the trap axis, the ion is confined in a DC potential well which is approximately harmonic with an oscillation frequency of $\omega_z \approx 300$ kHz. By applying asymmetric voltages, the minimum of the potential well, and thus the equilibrium position of the ion, is moved along the trap axis. By simultaneously monitoring the fluorescence, we sampled one-dimensional cross-sections of the cavity mode. The width of the ion's wave function in the axial potential well is a few hundred nanometres, which provides sufficient resolution to map the transverse mode pattern with an intensity distribution varying on a scale given by the cavity waist w_0 .

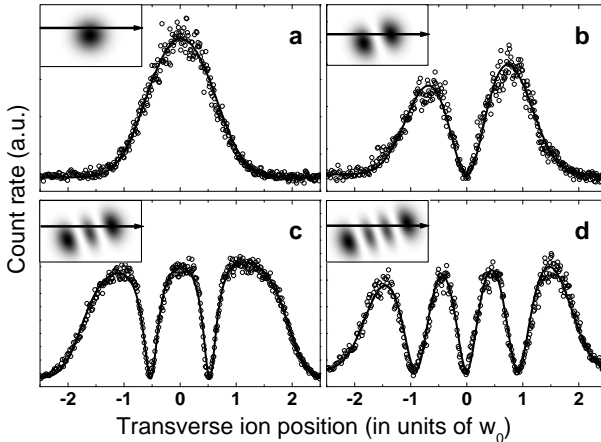


Figure 5: Transverse profiles of the Hermite-Gauss modes of the cavity, obtained by monitoring the ion's fluorescence while scanning over a range of $120 \mu\text{m}$. The solid line is a fit including saturation of the transition. The inset shows the calculated intensity distribution of the mode and indicates the scan path. The modes are a) TEM_{00} , b) TEM_{01} , c) TEM_{02} , d) TEM_{03} .

Figure 5 shows scans of the first four TEM_{0n} modes of the cavity obtained in this way. The fluorescence data are not entirely symmetric because of a small displacement and rotation of the cavity eigenmodes with respect to the trap axis. In each plot, an inset indicates the path along which the ion is scanned. The solid curves in Fig. 5 are obtained from a fit using Hermite-Gauss functions and take into account saturation of the ion's transition. The influence of saturation is apparent in Fig. 5c, where a slightly higher intensity was injected into the cavity. In all cases, the correspondence with the measured fluorescence is excellent.

The ion's motion must be restrained to the trap axis, since off the axis the radio-frequency field of the trap would lead to micromotion. To scan other dimensions of the field, the sample must be moved. In our experiment this is done by piezoelectrically translating the entire cavity assembly perpendicularly to the trap axis. In this way complete three-dimensional mapping of the mode field can be obtained [33].

RF confinement of the ion perpendicular to the trap axis is also harmonic, but the corresponding oscillation frequency $\omega_r \approx 1.1$ MHz is larger than the axial frequency so that field structures in the radial direction of the trap are better resolved. The

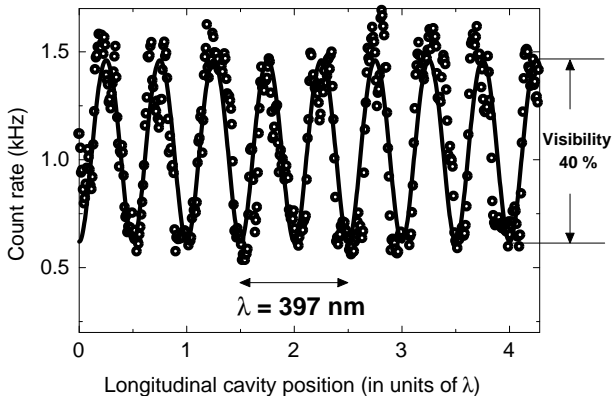


Figure 6: Single-ion mapping of the longitudinal structure of the cavity field. The visibility is determined by the residual thermal motion of the Doppler-cooled ion. It corresponds to a resolution of 60 nm. The localisation of the ion’s wave packet in this measurement is 16 nm.

resolution achieved by our method may be most accurately determined by probing the standing-wave field created between the cavity mirrors, which varies on a scale of $\lambda/2$. To this end, the cavity was moved parallel to its axis while keeping the ion stationary and monitoring its fluorescence. Figure 6 shows the mapping of the cavity field obtained in this way. A pronounced standing-wave pattern is observed with a visibility of 40 %. For details see also Ref. [33].

Taking advantage of the excellent localisation in ion traps, we performed the hitherto most precise measurement of a three-dimensional spatial structure of an optical field over a range of up to 100 μm . As a demonstration, we scanned modes of a low-loss optical cavity. The precise positioning we achieve implies deterministic control of the coupling between the ion and field. At the same time, the field and the internal states of the ion are not affected by the trapping potential. What we have realised, therefore, is an ideal system for cavity QED with a single particle.

2 Conclusion

This paper reviews our work on the generation of photon number states on demand by means of the micromaser. In addition, it describes first experiments using a single trapped ion in conjunction with an optical cavity. The two systems described show great promise and will afford a series of interesting new applications [27, 33].

References

- [1] D. Leibfried, D.M. Meekhof, B.E. King, C. Monroe, W. M. Itano, and D. J. Wineland, Phys. Rev. Lett **77**, 4281 (1996).
- [2] H. Zbinden, N. Gisin, B. Huttner, and W. Tittel, J. Cryptol. **13**, 207 (2000); H.-K. Lo and H. F. Chau, Science **283**, 2050 (1999).

- [3] K. M. Gheri, C. Saavedra, P. Törmä, J. I. Cirac, and P. Zoller, *Phys. Rev. A* **58**, R2627 (1998); S. J. van Enk, J. I. Cirac, and P. Zoller, *Phys. Rev. Lett.* **78**, 4293 (1997); S. J. van Enk, J. I. Cirac, and P. Zoller, *Science* **279**, 205 (1998).
- [4] J. I. Cirac, P. Zoller, H. J. Kimble, and H. Mabuchi, *Phys. Rev. Lett.* **78**, 3221 (1997); A. S. Parkins, P. Marte, P. Zoller, and H. J. Kimble, *Phys. Rev. Lett.* **71**, 3095 (1993); S. Parkins and H. J. Kimble, *J. Opt. B*, **1**, 496 (1999).
- [5] T. Jennewein, C. Simon, G. Weihs, H. Weinfurter, and A. Zeilinger, *Phys. Rev. Lett.* **84**, 4729 (2000); D. S. Naik, C. G. Peterson, A. G. White, A. J. Berglund, and P. G. Kwiat, *Phys. Rev. Lett.* **84**, 4733 (2000); W. Tittel, J. Brendel, H. Zbinden, and N. Gisin, *Phys. Rev. Lett.* **84**, 4737 (2000).
- [6] The error-tolerant quantum computing proposal by D. Gottesman, and I. L. Chuang, *Nature* **402**, 390 (1999), requires that a “quantum resource” be supplied *on demand* to facilitate computation. Such a source can be provided by the apparatus considered here. See also J. Preskill, *Nature* **402**, 357 (1999); D. Johnathon and M. B. Plenio, *Phys. Rev. Lett.*, **83**, 3566 (1999).
- [7] Sources of single atoms, such as that described in this paper, are routinely employed for hypothetical tasks such as creation of an atomic beam with arbitrary timing sequence or for stabilisation of cavity states. See, for example, D. Vitali, P. Tombesi, and G. Milburn, *Phys. Rev. A* **57**, 4930 (1998).
- [8] J. T. Höffges, H. W. Baldauf, W. Lange, and H. Walther, *J. Mod. Opt.* **44**, 1999 (1997).
- [9] F. Diedrich and H. Walther, *Phys. Rev. Lett.* **58**, 203 (1987).
- [10] J. T. Höffges, H. W. Baldauf, T. Eichler, S.R. Helmfrid, and H. Walther, *Opt. Comm.* **133** 170 (1997).
- [11] C. Brunel, B. Lounis, P. Tamarat, and M. Orrit, *Phys. Rev. Lett.* **83**, 2722 (1999).
- [12] C. K. Hong and L. Mandel, *Phys. Rev. Lett.* **56**, 58 (1986).
- [13] J. Kim, O. Benson, H. Kan, and Y. Yamamoto, *Nature* **397**, 500 (1999).
- [14] B. T. H. Varcoe, S. Brattke, M. Weidinger, and H. Walther, *Nature* **403**, 743 (2000).
- [15] M. Weidinger, B. T. H. Varcoe, P. Heerlein, and H. Walther, *Phys. Rev. Lett.* **82**, 3795 (1999).
- [16] G. M. Meyer, H.-J. Briegel, and H. Walther, *Europhys. Lett.* **37**, 317 (1997).
- [17] C. K. Law and J. H. Eberly, *Phys. Rev. Lett.* **76**, 1055 (1996); C. K. Law and H. J. Kimble, *J. Mod. Opt.* **44**, 2067 (1997); P. Domokos, M. Brune, J. M. Raimond, and S. Haroche, *Eur. Phys. J. D* **1**, 1 (1998).
- [18] See A. Kuhn, M. Hennrich, G. Rempe, *Phys. Rev. Lett.* **89**, 199 (2002) and references therein, e.g. A. Kuhn, M. Hennrich, T. Bondo, and G. Rempe, *Appl. Phys B* **69**, 373 (1999); P. W. H. Pinkse, T. Fischer, P. Maunz, and G. Rempe, *Nature* **404**, 365 (2000); J. Ye, D. W. Vernooy, and H. J. Kimble, *Phys. Rev. Lett.* **83**, 4987 (2000); C. J. Hood, T. W. Lynn, A. C. Doherty, A. S. Parkins, and H. J. Kimble, *Science* **287**, 1447 (2000).
- [19] See, for example, M.O. Scully and M. S. Zubairy, *Quantum Optics* (Cambridge University Press, 1997).

- [20] G. Rempe, F. Schmidt-Kaler, and H. Walther, *Phys. Rev. Lett.* **64**, 2783 (1990).
- [21] G. Rempe, H. Walther, and N. Klein, *Phys. Rev. Lett.* **58**, 353 (1987).
- [22] B. Englert, M. Löffler, O. Benson, M. Weidinger, B. Varcoe, and H. Walther, *Fortschr. Phys.* **46**, 897 (1998).
- [23] J. Krause, M.O. Scully, and H. Walther, *Phys. Rev. A* **36**, 4547 (1987).
- [24] G. Nogues, A. Rauschenbeutel, S. Osnaghi, M. Brune, J. M. Raimond, and S. Haroche, *Nature* **400**, 239 (1999).
- [25] A detailed account of the simulations used in this paper and a comparison with ideal micromaser theory are given in S. Brattke, B.-G. Englert, B. T. H. Varcoe, and H. Walther, *J. Mod. Opt.* **47**, 2857 (2000).
- [26] S. Brattke et al., *Optics Express* **8**, 131 (2001).
- [27] S. Brattke, B. T. H. Varcoe, and H. Walther, *Phys. Rev. Lett.* **86**, 3534 (2001).
- [28] Proposals such as teleportation of an atomic state using multiple atomic beams would be substantially enhanced if atoms arrived on demand rather than by chance. See, for example, L. Davidovich, M. Zagury, M. Brune, J. M. Raimond, and S. Haroche, *Phys. Rev. A* **50**, R895 (1994); J. I. Cirac and A. S. Parkins, *Phys. Rev. A* **50**, R4441 (1994); M. H. Y. Moussa, *Phys. Rev. A* **55**, R3287 (1997).
- [29] P. Lougowski, E. Solano, Z.M. Zhang, H. Walther, H. Mack, and W.P. Schleich, [quant-ph/0206083v1](https://arxiv.org/abs/quant-ph/0206083v1).
- [30] M. Hennrich, T. Legero, A. Kuhn, and G. Rempe, *Phys. Rev. Lett.* **85**, 4872 (2000).
- [31] T. Pellizzari, S. A. Gardiner, J. I. Cirac, and P. Zoller, *Phys. Rev. Lett.* **75**, 3788 (1995).
- [32] S. B. Zheng and G. C. Guo, *Phys. Rev. Lett.* **85**, 2392 (2000).
- [33] G. R. Guthöhrlein, M. Keller, K. Hayasaka, W. Lange, and H. Walther, *Nature* **414**, 49 (2001).